Crystal structure–solubility relationships in optical resolution by diastereomeric salt formation of DL-phenylglycine with (1*S*)-(+)-camphor-10-sulfonic acid

Ryuzo Yoshioka,*[a] Hajime Hiramatsu,[b] Kimio Okamura,[a] Ikuko Tsujioka[a] and Shin-ichi Yamada[a]

[a] *Product and Technology Development Laboratory, Tanabe Seiyaku Co., Ltd., 16-89, Kashima 3-Chome, Yodogawa-ku, Osaka 532-8505, Japan*
[b] *Discover Research Laboratory, Tanabe Seiyaku Co., Ltd., 16-89, Kashima 3-Chome, Yodogawa-ku, Osaka 532-8505, Japan*

Received (in Cambridge, UK) 17th April 2000, Accepted 11th July 2000
Published on the Web 7th September 2000

The experimentally-optimized optical resolution of DL-phenylglycine (PG) with (1*S*)-(+)-camphor-10-sulfonic acid ((+)-CS) afforded the crystalline D-PG·(+)-CS salt in 45.7% isolated yield and 98.8% optical purity. This excellent resolution has been studied by comparison of the crystal properties of the diastereomeric salt pair, D- and L-PG·(+)-CS. Thermoanalysis (DSC) of the less-soluble D-PG·(+)-CS showed a higher melting point and a larger enthalpy of fusion than those of the more-soluble L-PG·(+)-CS. The difference in the solubilities of the two salts in water is very large because the more-soluble L-PG·(+)-CS is freely soluble. The X-ray crystal structure of D-PG·(+)-CS shows a dense and stable molecular conformation of alternating PG cation layers and (+)-CS anion layers, whereas that of L-PG·(+)-CS shows a coarser molecular conformation consisting of characteristic "holey" vacancy layers, an important factor in its free solubility. The difference in the two characteristic structures could be closely related to the high efficiency of the resolution. A geometrical discussion of the (+)-CS molecule predicted that its excellent resolving ability may be due to its combining two structural functions; a hydrophilic flexible methanesulfonic acid site and a hydrophobic rigid camphor site.

Optical resolution through diastereomer formation, although referred to as a classical method, is one of the most convenient procedures available for separating enantiomers on both laboratory and industrial scales.[1] As a typical example of this technique, it has been well-known for many years that optically active D-phenylglycine (PG), which is an important raw material for the preparation of semisynthetic β-lactam antibiotics, can be prepared by diastereomeric resolution of DL-PG using (1*S*)-(+)-camphor-10-sulfonic acid ((+)-CS) as the resolving agent.[2] Up to quite recently, this resolution procedure was the main industrial production method for D-PG, due to its simplicity and very high yield.[3] We are interested in the chiral recognition mechanism that occurs during fractional crystallization of a diastereomeric salt pair, and would like to discover why the efficiency of the present resolution is so very good.

Recently, a few such diastereomeric resolutions have been investigated *via* comparisons between the physicochemical properties and crystal structures of a pair of diastereomeric salts.[4] The efficiency of the resolution process mainly depends on the difference in solubility of the diastereomeric salt pair in a solvent. We have been studying the characteristic differences between diastereomeric pairs through systematic resolutions of DL-amino acids with chiral sulfonic acids.[4k,5] The latter are also of interest for their optical resolution efficiency and in the design of new chiral resolving agents. In the present paper we try to further clarify the relationships between the resolving efficiency and the physicochemical properties, including the crystal structures, of the diastereomeric salt pair of DL-PG with (+)-CS by spectroscopic, DSC and X-ray crystallographic analyses.

Results and discussion

Optical resolution and characterization of DL-PG with (+)-CS

Although the optical resolution of DL-PG with (+)-CS is a known method,[2] a systematic investigation of it has not been reported. To understand in detail the efficiency of the present resolution, we have evaluated it under several resolution conditions; varying the amount of solvent and the molar ratio of (+)-CS and looking at the effect of additives (Table 1).

The optimum resolution of DL-PG with one equivalent of (+)-CS in water gave the less-soluble D-PG·(+)-CS salt in 44.1% yield (based on the DL-salt) and 86.0% optical purity (OP). Evidently, the addition of the mineral acid salts, sodium chloride or ammonium chloride, was found to increase the resolving efficiency (especially improving OP). Furthermore, an improved method, using 0.6 molar equivalents of (+)-CS, which is both economically and practically attractive gave 43% yield and 98% OP by both the addition of 0.55 molar equivalents of hydrochloride and a decrease in the amount of water. A scaled-up process based on such optimum conditions afforded D-PG·(+)-CS in up to 45.7% yield and 98.8% OP; that is, the observed resolving efficiency (RE) was 0.90.[6]

The above efficient resolution is presumed to be due to the large differences in the physicochemical properties (melting points, enthalpies of fusion, and solubilities) of the diastereomeric salt pair, D- and L-PG·(+)-CS. As shown in Table 2, the solubility of D-PG·(+)-CS, 5.7 g in 100 g water, is fairly low. Surprisingly, that of L-PG·(+)-CS can be as much as 150 g in 100 g water, which is very high (though not yet precisely determined). If the solubility of the L-salt was infinitely large in water, the present resolution (crystallization of the D-salt) would be perfectly achieved, except for contamination by a very small amount of the L-salt. Consequently, such a large difference in the solubilities between the two salts leads to an efficient resolution result.

Thermoanalysis of D- and L-PG·(+)-CS

Since the difference in solubilities of a diastereomeric salt pair is known to be closely associated with the difference in their

Table 1 Optical resolution of DL-PG with (+)-CS

Run	DL-PG/g	(+)-CS·H_2O/g	Additive			D-PG·(+)-CS			
			NaCl/g	12 M HCl/ml	H_2O/ml	Yield[g]/g (%)	$[\alpha]_D^{25}$ [h]	OP[i] (%)	RE[j]
1[a]	1.51	2.55	0	0	8	1.69(44.1)	−40.8	86.0	0.76
2	1.51	2.55	0.59	0	8	1.65(43.0)	−44.4	91.7	0.79
3	1.51	2.55	1.17	0	8	1.72(44.9)	−43.6	90.4	0.81
4	1.51	2.55	0.54[d]	0	8	1.68(43.8)	−42.7	89.0	0.78
5	1.51	2.55	1.07[d]	0	8	1.70(44.4)	−43.5	90.3	0.80
6	3.02	3.06[b]	0	1	8	3.31(43.1)	−48.4	97.9	0.86
7	3.02	3.06[b]	1.18	1	12	3.22(42.0)	−48.4	97.9	0.82
8	3.02	3.06[b]	1.18	1	10	3.46(45.1)	−42.2	88.2	0.80
9	7.56	13.62[c]	0	11[f]	19	8.85(46.2)	−46.1	94.0	0.87
10[a]	151.2	250.3	40[e]	220[f]	380	175.4 (45.7)	−48.4	98.8	0.90

[a] For details of these two procedures see Experimental section. [b] 0.6 equivalents for DL-PG. [c] Na salt of (+)-CS. [d] NH_4Cl (1 or 2 equivalents for DL-PG). [e] NaOH. [f] 5 M HCl. [g] Yield based on DL-salt. [h] *c* 2 in 1 M HCl. [i] (OP, %) Optical purity (OP%) of the salt (PG moiety) was calculated from the following specific rotations. D-PG·(+)-CS: $[\alpha]_D^{25}$ −49.7 (*c* 2 in 1 M HCl), DL-PG·(+)-CS: $[\alpha]_D^{25}$ +13.6 (*c* 2 in 1 M HCl). [j] Resolving efficiency (RE): 2(Yield)/100 × OP/100.

Table 2 Properties of D- and L-PG·(+)-CS

PG·(+)-CS	Mp[a]/°C	ΔH^f[a]/kJ mol^{-1}	Solubility[b]	$[\alpha]_D^{25}$[c]	C=O ν_{max}/cm^{-1}
D-PG·(+)-CS	207	(86.8)	5.75	−49.7	1740, 1725
L-PG·(+)-CS	191	(73.8)	>150	+74.9	1750, 1705

[a] DSC Mp: Peak maxima. DSC ΔH^f: Enthalpy of fusion. Parentheses indicate that the fusion process was accompanied by decomposition. [b] g per 100 g H_2O at 25 °C. [c] *c* 2 in 1 M HCl.

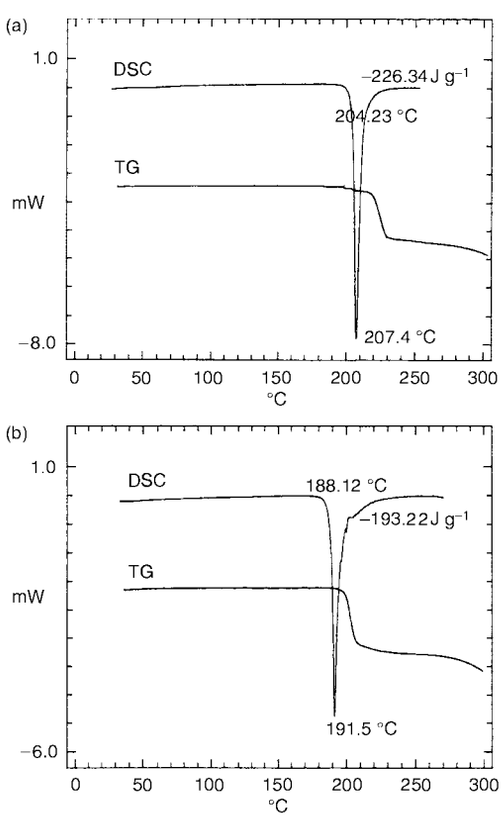

Fig. 1 DSC and TG curves of (a) D-PG·(+)-CS and (b) L-PG·(+)-CS.

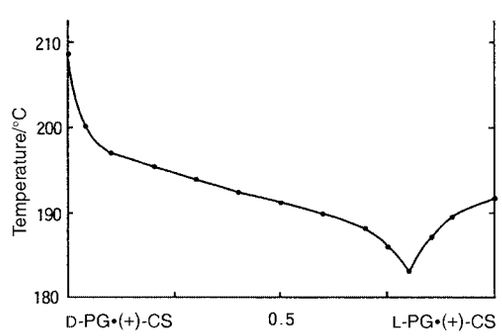

Fig. 2 Binary phase diagrams of the diastereomeric PG·(+)-CS salts.

melting points and enthalpies of fusion,[7] we have performed a thermoanalysis of the two salts.

By differential scanning calorimetry (DSC), the melting points of both the crystalline D- and L-PG·(+)-CS have a single endothermic peak due to fusion, with maxima at 207.4 and 191.5 °C, respectively, which are immediately accompanied by decomposition (Fig. 1). The difference in these two melting points could be approximately responsible for the difference in the two enthalpies of fusion, and also their differences could be attributed to the difference in the two solubilities described above.

Furthermore, although the DSC-melting points of both salts are accompanied by slight decompositions, we have illustrated a binary phase diagram using the melting points of moderate mixtures of the two diastereomeric salts; this is often used for evaluation of resolving efficiency.[7b,8] Twelve kinds of crystal mixtures, with different D-:L-salt component ratios, were prepared by grinding them to obtain homogeneous fine powders. Their mixture ratios were accurately analyzed by chiral HPLC. As illustrated in Fig. 2, plotting the DSC-melting points of these mixtures gave a binary phase diagram with a contact point for the two slope lines and its eutectic point at *ca.* 0.8, which indicates favorable resolution efficiency. Indeed, this point is in fair agreement with the results of the resolution experiments, that are RE = 0.76–0.90 (Table 1).

Crystal structures of the diastereomeric salts

Such large differences in the solubility and thermodynamic properties between the two diastereomeric salts led us to compare the crystal structures of the D- and L-PG·(+)-CS.

Fortunately, we were able to prepare suitable single crystals of both types for the X-ray crystallographic analyses, although those of L-PG·(+)-CS were not easy to prepare due to their very high solubility. The crystal data are listed in Table 3. Crystals of D-PG·(+)-CS are colorless needles in the orthorhombic

Table 3 Crystal and experimental data

	D-PG·(+)-CS	L-PG·(+)-CS
Formula	$C_{18}H_{25}NO_6S$	$C_{18}H_{25}NO_6S$
Formula weight	383.46	383.46
Crystal system	Orthorhombic	Monoclinic
Space group	$P2_12_12_1$	$P2_1$
Z	4	4
a/Å	17.527(2)	24.943(1)
b/Å	15.290(2)	7.053(2)
c/Å	6.912(1)	11.366(4)
β/deg		103.39(3)
V/Å^3	1852.3(4)	1945.2(8)
Dx/g cm^{-3}	1.375	1.309
μ (Cu-Kα)/mm^{-1}	1.859	1.770
No. of reflections used ($I > 2\ \sigma(I)$)	1495	1451
No. of parameters:	236	235
R	0.054	0.060
Rw	0.155	0.154
Goodness-of-fit	1.02	1.00
ρ max/min/eÅ^{-3}	0.76/−0.49	0.31/−0.73

Table 4 Selected torsion angles (°) of the diastereomeric salts

	D-PG· (+)-CS	L-PG· (+)-CS	L-PG and (+)-CS
PG			(L-PG)[a]
O(34)–C(33)–C(32)–N(31)	12(10)	3.7(10)	−18.35
O(34)–C(33)–C(32)–C(36)	−112.0(7)	127.5(8)	104.05
O(35)–C(33)–C(32)–N(31)	−169.1(5)	−178.9(6)	162.47
O(35)–C(33)–C(32)–C(36)	66.8(6)	−55.1(8)	−75.13
N(31)–C(32)–C(36)–C(37)	127.2(5)	−107.8(7)	−129.61
N(31)–C(32)–C(36)–C(41)	−54.9(6)	72.5(8)	55.64
C(32)–C(36)–C(37)–C(38)	177.3(5)	176.5(7)	−174.78
C(32)–C(36)–C(41)–C(40)	−178.1(5)	−178.8(9)	174.59
C(33)–C(32)–C(36)–C(37)	−111.4(5)	129.5(7)	110.46
C(33)–C(32)–C(36)–C(41)	66.5(6)	−50.3(9)	−64.27
(+)-CS			((+)-CS)[b]
S(1)–C(5)–C(6)–C(7)	−100.3(6)	174.8(7)	−115.52
S(1)–C(5)–C(6)–C(12)	23.8(7)	−71.7(8)	1.52
S(1)–C(5)–C(6)–C(13)	145.8(4)	58.1(9)	125.29
O(8)–C(7)–C(9)–C(10)	−175.5(6)	178.0(1)	−175.25
C(5)–C(6)–C(7)–C(9)	−158.1(7)	−165.9(7)	−160.91
C(5)–C(6)–C(13)–C(10)	176.1(7)	173.9(6)	176.74
C(6)–C(7)–C(9)–C(10)	1.1(7)	−0.4(9)	−2.17
C(6)–C(12)–C(11)–C(10)	3.1(7)	4.2(7)	4.05
C(7)–C(6)–C(12)–C(11)	−71.1(7)	−71.9(6)	−73.16
C(7)–C(6)–C(13)–C(15)	171.1(7)	167.9(6)	169.87
C(9)–C(10)–C(11)–C(12)	69.1(7)	69.8(6)	70.42
C(11)–C(10)–C(13)–C(15)	−62.1(7)	−63.6(7)	−61.44
C(12)–C(6)–C(13)–C(14)	−170.1(7)	−169.3(6)	−169.77

[a] Torsion angles of L-PG·HCl, see references 9 and 10. [b] Torsion angles of quinoline·(+)-CS salt in the literature, see reference 11.

$P2_12_12_1$ space group, and those of L-PG·(+)-CS are colorless needles in the monoclinic $P2_1$ space group. The unit cells of both salts contain four PG cations and four (+)-CS anions. The atomic-numbering schemes are graphically illustrated in Figs. 3(a) and 4(a). Tables of the final positional and thermal parameters, and lists of the bond lengths, bond angles, and coordinates of the calculated hydrogen positions have been deposited.[9]

Stereochemistry of the diastereomeric salts

One of our interests during this study was to explore the geometric and functional roles of a resolving agent during diastereomeric salt formation (crystallization). Thus, the conformations of the D- or L-PG and (+)-CS molecules on the two crystal structures have been investigated by comparing their torsion angles (Table 4).

The molecular geometries of the PG cations can be mainly correlated to the torsion angles of O(34)–C(33)–C(32)–N(31), O(34)–C(33)–C(32)–C(36), N(31)–C(32)–C(36)–C(37) and C(33)–C(32)–C(36)–C(37). The variations in the torsion angles between the D- and L-PG molecules are not significant, being no more than 20° different, except for the difference (mirror image) in the D/L configuration on the chiral carbon atom [(C(32)]. The torsion angles of the two PG molecules also moderately agree with those of crystalline L-PG·HCl salt,[9,10] some of which are shown in Table 4. The two sets of bond lengths, which are essentially similar, are also in fair agreement with those of the L-PG·HCl salt. These observations suggest that the molecular geometries of both D- and L-PG are not strikingly deformed during crystallization based on optical resolution.

The torsion angles of the (+)-CS molecules are shown in Table 4, and are compared with the corresponding values for another (+)-CS salt.[11] The structure of the CS anion can be considered by looking separately at the camphor and methanesulfonic acid groups. The camphor species, C(5)–C(6)–C(13)–C(10), C(6)–C(7)–C(9)–C(10) and C(6)–C(12)–C(11)–C(10), have similar torsion angles in the two salts. This camphor structure is very rigid and stable, because its cyclohexyl ring, C(6)–C(7)(–O(8))–C(9)–C(10)–C(11)–C(12), is supported by C(6)–C(13)(–C(14),–C(15))–C(10) bridge bonds. In contrast, the methanesulfonic acid moiety, C(6)–C(5)–S(1), shows large differences in torsion angles for both salts, so the camphor and sulfonic acid sites around the C(5) atom must be very flexible (Fig. 5).

These observations suggest that in the formation of the salts during optical resolution, it is the molecular geometry of the (+)-CS that is deformed, whereas the PG molecule is relatively rigid and stable.

Conformational role of (+)-CS as a resolving agent

Since the functional role of (+)-CS as a resolving agent is very interesting, we have studied and compared the molecular geometries of other resolution examples using (+)-CS. Two recent reports showed common characteristics,[11,12] similar to those described above; that is, the conformation of the camphor group site remains approximately the same, while that of the methanesulfonic acid group site displays significant variation. Therefore, the key structural features the (+)-CS molecule possesses seem to be a hydrophilic flexible methanesulfonic acid site and a hydrophobic rigid camphor site. Presumably, when the salt of (+)-CS is formed with a basic compound, the flexible site plays a minor role in the formation of the more stable molecular structure and the rigid site helps in accelerating the crystallization. This makes (+)-CS a useful resolving agent for various racemic basic compounds.[13]

Hydrogen bonds and crystal packing structures

Typical crystal packing structures of D- and L-PG·(+)-CS are shown in Figs. 3 and 4, respectively. These packing forms are the acid–base complex structures consisting of the carboxylate and ammonium groups of the PG cations with the sulfonium groups of the (+)-CS anions, supported by electrostatic interaction and hydrogen-bonding, together with van der Waals interactions. The hydrogen bonds are listed in Table 5.

In the crystal packing of the less-soluble D-PG·(+)-CS [Fig. 3(c)], there is a characteristic hydrogen-bond network, mainly formed by the PG ammonium and carboxylate oxygen with the adjacent (+)-CS sulfonium oxygen and carbonyl oxygen; namely, the PG ammonium (N(31)) forms three normal hydrogen bonds, (N(31)–O(2), 2.841; N(31)–O(3), 2.947; and N(31)–O(4), 2.787 Å) with the sulfonium oxygens of the three adjacent CS, and, additionally, the PG carboxylate (O(35)) links a short hydrogen bond (O(35)–O(8), 2.682 Å) with the adjacent CS carbonyl oxygen (O(8)). These hydrogen bonds form a striking spiral zigzag-type line, extending infinitely along the a-axis. Also, viewed from the b- or c-axis direction, the D-PG and (+)-CS layers seem to be in an alternate arrangement [Fig. 3, (b) and (c)]; there are strongly hydrophobic layers. In contrast, a

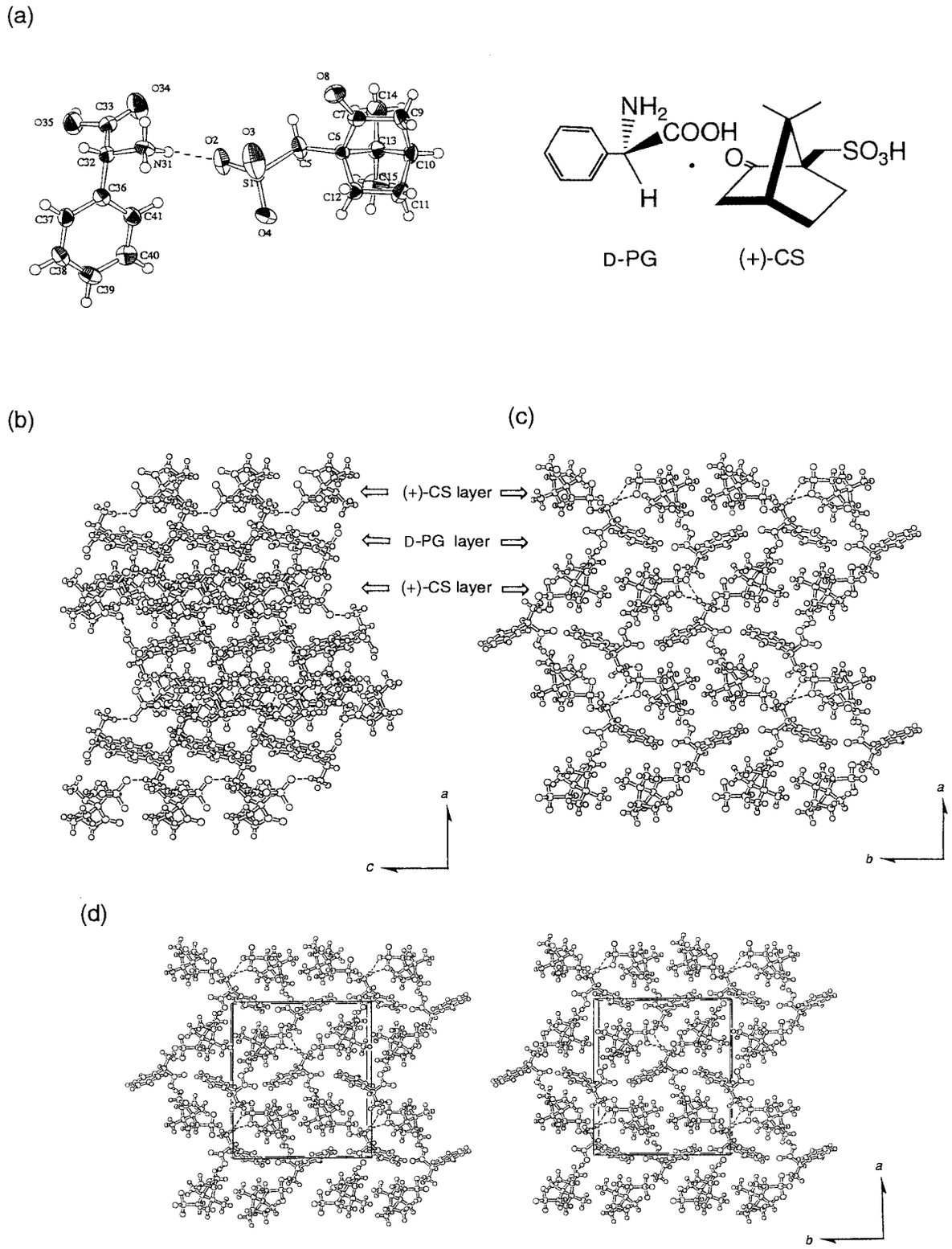

Fig. 3 (a) ORTEP view of D-PG·(+)-CS with atomic numbering. Displacement ellipsoids are drawn at the 50% probability level. (b) Unit cell and the lattice arrangement of D-PG·(+)-CS viewed down the *b*-axis. Broken lines denote hydrogen bonds. Directions of the three arrows show alternate D-PG and (+)-CS layers. (c) Viewed down the *c*-axis. (d) Stereoview of the hydrogen-bonding network viewed down the *c*-axis.

definite hydrophilic region could not be found in that direction. Therefore, the main structural characteristic of the less-soluble salt seems to be that the arrangement of the D-PG and (+)-CS molecules is quite homogeneous and balanced, and the entire crystal structure is densely packed. Such a molecular arrangement mode will apparently induce a strong hydrophobic effect, thus resulting in the observed low solubility.

In the crystal packing of the more-soluble L-PG·(+)-CS [Fig. 4(c)], a characteristic helical hydrogen-bond network is observed. The PG ammonium (N(31)) forms three hydrogen bonds, (N(31)–O(2), 2.781; N(31)–O(3), 2.828; and N(31)–O(8), 2.787 Å) with the sulfonium oxygens of the two adjacent CS and with the adjacent CS carbonyl oxygen, respectively, and, additionally, the same PG carboxylate (O(35)) links a short hydrogen bond (O(35)–O(4), 2.602 Å) with the adjacent CS sulfonium oxygen (O(4)). These hydrogen-bonding chains extend in parallel along the *c*-axis direction, forming the two L-PG and two (+)-CS units related to a two-fold screw

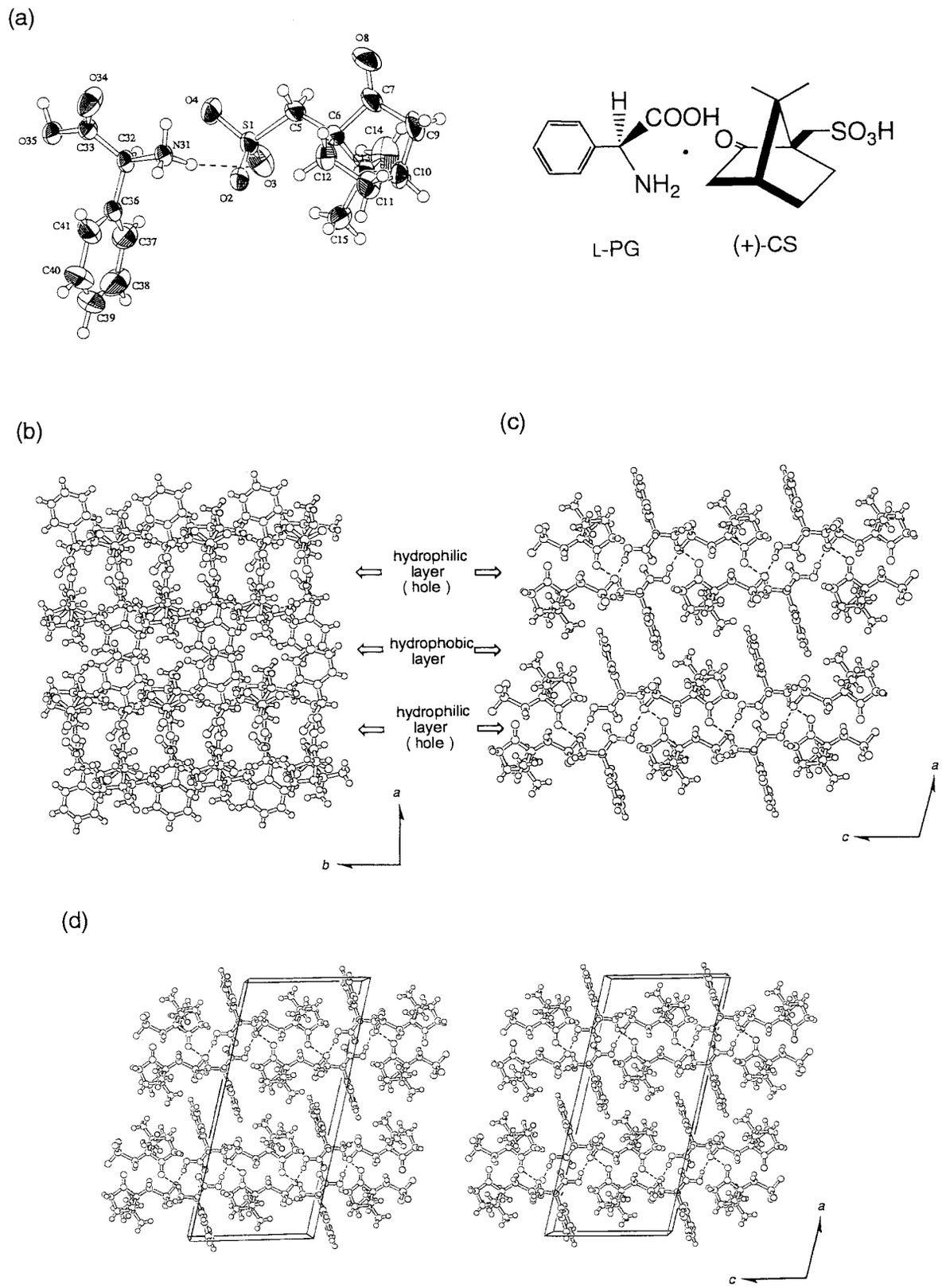

Fig. 4 (a) ORTEP view of L-PG·(+)-CS with atomic numbering. Displacement ellipsoids are drawn at the 50% probability level. (b) Unit cell and the lattice arrangement of L-PG·(+)-CS viewed down the *c*-axis. Broken lines denote hydrogen bonds. Directions of the arrows show alternate charged ions layers (hole: a tunnel image) and phenyl–camphor mixed layer. (c) Viewed down the *b*-axis. (d) Stereoview of the hydrogen-bonding network viewed down the *b*-axis.

axis. Additionally, when the hydrogen-bonding column is viewed from the *c*-axis direction, as shown in Fig. 4, (b) and (c), a sectional view of the structure seems to be a hydrophobic layer, consisting of the phenyl and camphor groups, alternating with a hydrophilic layer, consisting of the charged ions parts; this entire packing structure is relatively looser and coarser, compared with that of the less-soluble D-PG·(+)-CS. Of note is that the L-PG salt's hydrophilic layers have large "holey" vacancies, consisting of an ellipse with a diameter *ca.* 10 Å over towards the *c*-axis direction, which are large enough for them to be easily invaded by water molecules. Such characteristic holes in the charged ion moieties seem to be an important factor in the salt's very high solubility.

Table 5 Geometry of interatomic hydrogen bonds

D–H · · · A	SYM[a]	Distance/Å	∠D–H · · · A/°
D-PG·(+)-CS			
[b]N(31) O(34)		2.691(5)	90.678
N(31) O(2)		2.841(5)	165.064
N(31) O(3)	2	2.947(5)	130.519
N(31) O(4)	2	3.206(8)	162.083
N(31) O(4)	3	2.787(6)	146.523
O(35) O(8)		2.682(5)	
L-PG·(+)-CS			
[b]N(31) O(34)		2.667(6)	102.042
N(31) O(2)	1	2.781(6)	167.207
N(31) O(4)	1	3.130(7)	109.755
N(31) O(3)	4	2.828(6)	154.483
N(31) O(8)	5	2.787(4)	139.380
O(35) O(4)		2.602(5)	

[a] SYM: Symmetry coord 1; x, y, z: 2; $-x + 1/2$, $-y$, $z + 1/2$: 3; x, y, $z + 1:4$; x, $y + 1$, z: 5; $-x + 3/2$, $y + 1/2$, $-z + 1$. [b] Intramolecular H-bonds.

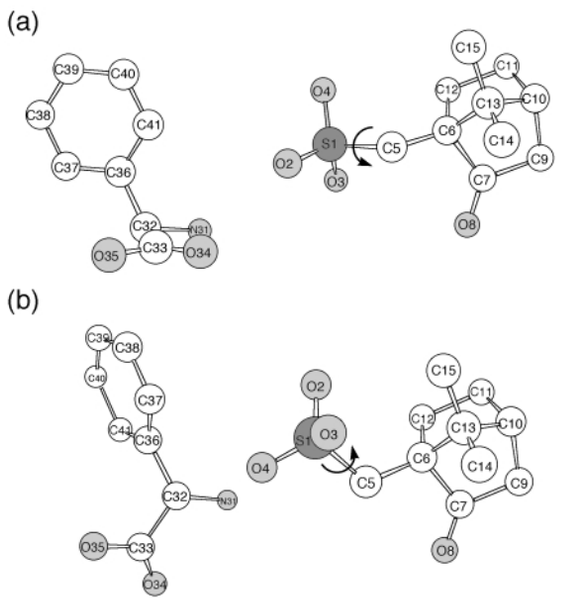

Fig. 5 Molecular geometries of (a) D-PG·(+)-CS and (b) L-PG·(+)-CS (when both camphor moieties are the same direction).

What is the relation between the structure and solubility?

It has become obvious that the successful resolution of DL-PG with (+)-CS can be attributed to the striking differences in both the physicochemical properties and crystal structures of the diastereomeric salt pair, which could be responsible for the large difference in the two solubilities. Such a clear difference is rare, although slight differences in diastereomeric pairs were usually observed in our studies and the literature.[4] In particular, it is noteworthy that the observation of the characteristic holes in the electrostatic moieties of the crystal structure of the more-soluble L-PG·(+)-CS, to our knowledge, is the first such discovery. The innumerable holes in the crystal structure are like a honeycomb, and are apparently related to the salt's unlimited solubility. It is, therefore, tempting to speculate that such a "holey" structure is an essential factor for achieving very successful resolution in an aqueous solvent. At present, a few other examples are being prepared to test this theory.

Another interesting phenomenon is the effect of additives on the optical resolution,[14] which appear to improve resolution efficiencies *via* diastereomeric resolution, as well as the preferential crystallization of enantiomers. As can be seen in Table 1, the addition of mineral acid salts constantly improved the resolution efficiencies (especially the increase in optical purity). This phenomenon can be explained by the simple presumption that when D-PG·(+)-CS is preferentially crystallized from the racemate solution, the added salt inhibits the crystallization of the more-soluble L-PG·(+)-CS; that is, the dissociated ions of the added salt interfere with the association between the major D-PG·(+)-CS and the minor L-PG·(+)-CS in water. In the present case, the "holey" structure of L-PG·(+)-CS appears to strengthen the effect of the additive. However, in addition to the difficulty in the separation of diastereomers, it is also difficult to prove a structural mechanism for the addition effect of a salt.

In an interesting connection with a PG derivative, the molecular geometry of PG is moderately similar to that of *p*-hydroxyphenylglycine (HPG), observed previously.[4k,5] However, HPG seems to be somewhat more flexible than PG. Probably, this slight difference is due to the presence of the *p*-hydroxy group on the phenyl ring of HPG. Interestingly, DL-HPG could not be resolved with (+)-CS, due to poor crystallization of the corresponding diastereomeric salt. This factor might be because both HPG and (+)-CS have a flexible group site. At least, it is clear that the *p*-hydroxy group of HPG plays an important role in the formation of the crystal structure. Such a subtle phenomenon is noteworthy, in common with recent papers reporting that the position and presence of a substituent on the phenyl ring of a resolving agent have a strong influence on the resolution efficiency and the crystal structure formation.[4i,n,15]

On the other hand, we have previously succeeded in the diastereomeric resolution of synthesized DL-HPG using (1*R*)-(+)-3-bromocamphor-9-sulfonic acid (BCS) as a resolving agent.[16] The molecular structures of HPG and BCS are analogous to PG and CS, respectively. Therefore, we are currently investigating the physicochemical properties and X-ray crystal structures of the diastereomeric salt pair D- and L-HPG·(+)-BCS, to compare them with those of the PG·(+)-CS mentioned above. From these studies, we expect to clarify the role and ability of optically active camphorsulfonic acid as a resolving agent.

Experimental

Methods

Differential-scanning calorimetric (DSC) traces were recorded on a Shimadzu DSC-50 system. Samples (2–5 mg) were sealed in aluminium lid-perforated pans. The temperature ranges were from ambient to approximately the decomposition of the salts at a heating rate of 5 °C min^{-1} under N_2 gas (30 ml min^{-1}). The DSC temperatures cited in this paper correspond to the peak maxima. Thermogravimetric (TG) traces were recorded on a Shimadzu TGA-50 system under similar conditions. Melting points were determined with a Yamato Mp-21 apparatus and are uncorrected. IR spectra were recorded on a Perkin-Elmer 1600-series FTIR spectrophotometer using KBr disks. ^{1}H NMR spectra were determined with a Bruker AC-200 (200 MHz) spectrometer. Optical rotations were measured on a Perkin-Elmer 341 automatic polarimeter. Values of specific rotation are given in deg cm^3 g^{-1} dm^{-1}. Elemental analyses were done using a Perkin-Elmer 2400 elemental analyzer. The solubilities were determined by approaching saturation equilibrium from both undersaturation and supersaturation. The solute concentrations were determined using a Waters Symmetry™ column (4.6 × 150 mm) with a Shimadzu LC-10A HPLC system equipped with an SPD-10A UV detector. Chiral analytical HPLC was carried out using a Daicel Crownpak CR (aqueous $HClO_4$, pH 2) with the detector wavelength at 254 nm.

Materials

Optically active and racemic phenylglycine (PG) were obtained from Tanabe Seiyaku, Co., Ltd. (1*S*)-(+)-Camphor-10-sulfonic

acid ((+)-CS) was obtained from Tokyo Kasei Kogyo Co., Ltd., and used without further purification.

Optical resolution of DL-phenylglycine with (1*S*)-(+)-camphor-10-sulfonic acid

(1) A standard example is as follows (Run 1 in Table 1). DL-PG (1.51 g, 10 mmol) was stirred in hot water (8 ml), and (+)-CS·H_2O (2.55 g, 10.2 mmol) was added. The clear solution was seeded with pulverized crystals of authentic D-PG·(+)-CS, slowly cooled to room temperature with stirring, and kept at 8 °C for 2 h. The precipitated crystals were filtered and washed with a small amount of cold water, and dried at 80 °C for 5 h to give crude D-PG·(+)-CS (1.69 g), yield 44.1% (based on starting DL-salt), $[a]_D^{25}$ −40.8 [*c* 2 in 1 mol dm^{-3} aq. HCl (1 M HCl)], optical purity 86.0%.

(2) A large-scale example is as follows (Run 10 in Table 1). DL-PG (151.2 g, 1 mol) was dissolved in 5 M HCl (220 ml) at elevated temperature, and a solution of (+)-CS·H_2O (250.3 g, 1 mol) and sodium hydroxide (40 g) in water (380 ml) was added. The clear solution was seeded with pulverized crystals of authentic D-PG·(+)-CS, slowly cooled to room temperature with stirring, and kept at 8 °C for 2 h. The precipitated crystals were filtered and washed with a small amount of cold water, and dried at 80 °C for 5 h to give crude D-PG·(+)-CS (175.4 g), yield 45.7% (based on starting DL-salt), $[a]_D^{25}$ −48.4 (*c* 2 in 1 M HCl), optical purity 98.8%. The resulting crude salt was purified by crystallization from water to afford the diastereomerically pure D-PG·(+)-CS (155.3 g, 88.5%); $[a]_D^{25}$ −49.7 (*c* 2 in 1 M HCl), optical purity 100%. An ee% of the salt (PG moiety) was determined to be >99% by chiral HPLC (a Daicel Crownpak CR(+) column).

Preparation and characterization of diastereomerically pure D- and L-PG·(+)-CS

The title compounds were prepared by the salt formation of optically pure D- and L-PG with (+)-CS.

D-PG·(+)-CS. A solution of D-PG (2.0 g, 13.2 mmol) and (+)-CS·H_2O (3.2 g, 14.9 mmol) dissolved in hot water was treated with active charcoal and evaporated to dryness under reduced pressure. After the resulting crude D-PG·(+)-CS was dissolved in water (25 ml) by heating, the solution was kept at room temperature for 10 days. The precipitated crystals were filtered by suction, washed with a small amount of cold water, and dried to give D-PG·(+)-CS (3.54 g), mp 211–212 °C, $[a]_D^{25}$ −49.7 (*c* 2 in 1 M HCl), $[a]_D^{25}$ −48.4° (*c* 1 in MeOH). ν_{max}(KBr)/cm^{-1} 3400, 2940, 1740, 1725, 1515, 1180, 880 and 700. δ_H(200 MHz; d_6-DMSO; Me_4Si) 0.74 (3H, s, CH_3), 1.05 (3H, s, CH_3), 1.27 (q, 2H, q, *J* 11 Hz, CH_2), 1.75–1.96 (3H, m, $CHCH_2$), 2.18–2.92 (4H, m, $CH_2 \times 2$), 5.12 (1H, s, CH), 7.47 (4H, m, Ar H) and 8.74 (3H, br s, NH_3^+). Anal. Calcd for $C_{18}H_{25}NO_6S$: C, 56.38; H, 6.57; N, 3.65; S, 8.36%. Found: C, 56.30; H, 6.54; N, 3.59; S, 8.38%.

L-PG·(+)-CS. A solution of L-PG (2.0 g, 13.2 mmol) and (+)-CS·H_2O (3.2 g, 14.9 mmol) dissolved in hot water was treated with active charcoal and evaporated to dryness under reduced pressure. The resulting oily residue was dissolved in acetonitrile and then seeded with L-PG·(+)-CS crystals. The precipitated crystals were filtered by suction, washed with a small amount of acetonitrile, and dried to give crude L-PG·(+)-CS (4.96 g), which was recrystallized from acetonitrile–MeOH (little) to afford L-PG·(+)-CS (3.90 g), mp 187–188 °C, $[a]_D^{25}$ +74.9 (*c* 2 in 1 M HCl), $[a]_D^{25}$ +97.9 (*c* 1 in MeOH). ν_{max}(KBr)/cm^{-1} 3440, 2950, 1750, 1705, 1520, 1165, 1045 and 765. ^{1}H NMR spectra of L-PG·(+)-CS were identical to that of D-PG·(+)-CS within experimental error. Anal. Calcd for $C_{18}H_{25}NO_6S$: C, 56.38; H, 6.57; N, 3.65; S, 8.36%. Found: C, 56.40; H, 6.60; N, 3.65; S, 8.40%.

X-Ray crystal structure determination[9]

The single crystals of each salt were grown from the same solvent system as that used in the optical resolution. All of the intensity data were collected on a AFC5R diffractometer (Rigaku) using graphite monochromated Cu-Kα (λ = 1.5418 Å) radiation. The data were corrected for Lorentz and polarization effects, but not for absorption. The program used was TEXSAN[17] of the SGI version. The structures were solved by a direct method using SHELXS-97,[18] and structure refinements on F^2 were carried out using SHELXL-97 with anisotropic temperature factors for all non-hydrogen atoms. All hydrogen atoms were found in a difference Fourier map, and were refined riding with the atoms to which they were bonded. The crystal data and final results are summarized in Table 3. ORTEP plots of the two salts are shown in Figs. 3(a) and 4(a), respectively.[19]

Acknowledgements

The authors are grateful to the staff and managing directors of our company for their encouragement and interest in the present study.

References and notes

1 (*a*) J. Jacques, A. Collet and S. H. Wilen, *Enantiomers*, *Racemates*, *and Resolutions*, Krieger Publishing Company, Malabar, Florida, 1994; (*b*) E. L. Eliel, S. H. Wilen and L. N. Mander, *Stereochemistry of Organic Compounds*, John Wiley and Sons, New York, 1994.
2 (*a*) M. Betti and M. Mayer, *Ber.*, 1908, **41**, 2071; (*b*) A. W. Ingersoll and R. Adams, *J. Am. Chem. Soc.*, 1922, **44**, 2930; (*c*) A. W. Ingersoll, *J. Am. Chem. Soc.*, 1925, **47**, 1168.
3 (*a*) J. Crosby, *Tetrahedron*, 1991, **47**, 4789; (*b*) A. N. Collins, G. N. Sheldrake and J. Crosby, *Chirality in Industry*, John Wiley and Sons, Chichester, England, 1992; (*c*) S. Kotha, *Tetrahedron*, 1994, **50**, 3639; (*d*) A. Collet, *Enantiomer*, 1999, **4**, 157.
4 For examples see: (*a*) M. C. Brianso, *Acta Crystallogr.*, *Sect. B*, 1981, **B37**, 618; (*b*) R. O. Gould and M. D. Walkinshaw, *J. Am. Chem. Soc.*, 1984, **106**, 7840; (*c*) R. O. Gould, R. Kelly and M. D. Walkinshaw, *J. Chem. Soc.*, *Perkin Trans. 2*, 1985, 847; (*d*) E. Fogassy, M. Ács, F. Faigl, K. Simon, J. Rohonczy and Z. Ecsery, *J. Chem. Soc.*, *Perkin Trans. 2*, 1986, 1881; (*e*) A. M. G. Kok, H. Wynberg, J. M. M. Smits, P. T. Beurskens and V. Parthasarathi, *Acta Crystallogr.*, *Sect. C*, 1987, **43**, 1328; *Acta Crystallogr.*, *Sect. C*, 1987, **43**, 1331; *Acta Crystallogr.*, *Sect. C*, **43**, 1336; (*f*) S. P. Zingg, E. M. Arnett, A. T. McPhail, A. A. Bothner-By and W. R. Gilkerson, *J. Am. Chem. Soc.*, 1988, **110**, 1565; (*g*) A. D. van der Haest, H. Wynberg, F. J. J. Leusen and A. Bruggink, *Recl. Trav. Chim. Pays-Bas*, 1990, **109**, 523; (*h*) F. Faigl, K. Simon, A. Lopata, É. Kozsda, R. Hargitai, M. Czugler, M. Ács and E. Fogassy, *J. Chem. Soc.*, *Perkin Trans. 2*, 1990, 57; (*i*) F. J. J. Leusen, H. J. Bruins Slot, J. H. Noordik, A. D. van der Haest, H. Wynberg and A. Bruggink, *Recl. Trav. Chim. Pays-Bas*, 1991, **110**, 13; (*j*) S. Kuwata, J. Tanaka, N. Onda, T. Yamada, T. Miyazawa, M. Sugiura, Y. In, M. Doi, M. Inoue and T. Ishida, *Bull. Chem. Soc. Jpn.*, 1993, **66**, 1501; (*k*) R. Yoshioka, O. Ohtsuki, T. Da-te, K. Okamura and M. Senuma, *Bull. Chem. Soc. Jpn.*, 1994, **67**, 3012; (*l*) K. Kinbara, K. Sakai, Y. Hashimoto, H. Nohira and K. Saigo, *J. Chem. Soc.*, *Perkin Trans. 2*, 1996, 2615; (*m*) M. R. Caira, R. Clauss, L. R. Nassimbeni, J. L. Scott and A. F. Wildervanck, *J. Chem. Soc.*, *Perkin Trans. 2*, 1997, 763: (*n*) K. Kinbara, Y. Kobayashi and K. Saigo, *J. Chem. Soc.*, *Perkin Trans. 2*, 1998, 1767.
5 R. Yoshioka, M. Tohyama, O. Ohtsuki, S. Yamada and I. Chibata, *Bull. Chem. Soc. Jpn.*, 1987, **60**, 649.
6 The efficiency of the optical resolution (RE) has been defined using the chemical yield (*Y*%) and the optical purity (OP% or ee%) as the following equation: 2*Y*/100 × OP/100.
7 (*a*) J. H. Hildebrand, *Solubility of Non-electrolytes*, 2nd edn., Reinhold Publishing Corporation, New York, 1936; (*b*) S. H. Wilen, A. Collet and J. Jacques, *Tetrahedron*, 1977, **33**, 2725; (*c*) D. Kozma, G. Pokol and M. Ács, *J. Chem. Soc.*, *Perkin Trans. 2*, 1992, 435.
8 E. J. Ebbers, B. J. M. Plum, G. J. A. Ariaans, B. Kaptein, Q. B. Broxterman, A. Bruggink and B. Zwanenburg, *Tetrahedron: Asymmetry*, 1997, **24**, 4047.
9 CCDC reference number 188/260. See http://www.rsc.org/suppdata/p2/b0/b003068f for crystallographic files in .cif format.

10 X-Ray crystal structure determination of L-PG·HCl. Crystal data: $C_8H_{10}ClNO_2$, $Fw = 187.62$, space group $P2_12_12_1$, $a = 7.2609(13)$, $b = 22.7812(19)$, $c = 5.4382(12)$ Å, $U = 899.5(3)$ Å^3, $F(000) = 392$, $Z = 4$, $Dx = 1.385$ Mg m^{-3}. The final R indices for reflection with $I > 2\sigma(I)$ were $R_1 = 0.026$, $wR_2 = 0.1022$.
11 Y. Hashimoto, Y. Okaichi, D. Nomi, H. Miyamoto, M. Bando, M. Kido, T. Fujimura, T. Furuta and J. Minamikawa, *Chem. Pharm. Bull.*, 1996, **44**, 642.
12 A. A. D'Souza, M. Motevalli, A. J. Robinson and P. B. Wyatt, *J. Chem. Soc.*, *Perkin Trans. 1*, 1995, 1.
13 P. Newman, *Optical Resolution Procedures for Chemical Compounds,* Optical Resolution Information Center, New York, 1978, vol. 1; P. Newman, *Optical Resolution Procedures for Chemical Compounds,* Optical Resolution Information Center, New York, 1981, vol. 2.
14 (*a*) T. Ogawa, *Kogyo Kagaku Zasshi*, 1949, **52**, 102; (*b*) T. Akaishi, *Nippon Kagaku Kaishi*, 1962, **83**, 421; (*c*) N. Mizoguti, *Nippon Nogei Kagaku Kaishi*, 1967, **41**, 616; (*d*) S. Asai and S. Ikegami, *Ind. Eng. Chem. Fundam.*, 1982, **21**, 181.
15 F. J. J. Leusen, H. J. Bruins Slot, J. H. Noordik, A. D. van der Haest, H. Wynberg and A. Bruggink, *Recl. Trav. Chim. Pays-Bas*, 1992, **111**, 111.
16 S. Yamada, C. Hongo, R. Yoshioka and I. Chibata, *Agric. Biol. Chem.*, 1979, **43**, 395.
17 TEXSAN: Single Crystal Structure Analysis Software, Version 1.10, 1999. Molecular Structure Corporation, The Woodland, TX, 77381.
18 G. M. Sheldrick, SHELXL-97: *Program for crystal structure refinement*, University of Göttingen, Germany, 1997.
19 C. K. Johnson, ORTEP II, Report ORNL-5138, Oak Ridge National Laboratory, Oak Ridge, TN, USA, 1976.